Forced vibrations of a finite length metabeam with periodically arranged internal hinges and external supports

K.Ghazaryan[a], G. Piliposyan[a], S. Jilavyan[b], G. Piliposian[c,*]

[a] *Institute of Mechanics, 24 Bagramyan ave., 0019 Yerevan*
[b] *Yerevan State University, Alek Manoogian 1, Yerevan*
[c] *University of Liverpool, Liverpool L69 3BX*

Abstract

The paper investigates a problem of forced vibrations of two finite length metabeams: one is with periodically arranged internal hinges and the second one with periodically arranged internal hinges and external supports. Based on the Euler-Bernoulli beam theory and the transfer matrix method, general solutions of the periodic beams are obtained. Applying the Bloch-Floquet theory, the explicit expressions are derived defining the metabeams band gap structures. The corresponding band gap dispersion curves are plotted and analysed. It is shown that when the frequency of forced vibrations coincides with the band gap frequencies a strong localization of flexible waves occurs at the interfaces of the periodic beams. The localization of flexible waves increases significantly with the number of hinges and supports.

Keywords: `Band gaps, localization, resonance frequency`

1. Introduction

Artificial materials and structures, called mechanical metamaterials, recently have received much attention in many research studies and engineering applications [1, 2]. Due to structural or material periodicity these materials possess new physical properties including negative refraction, frequency stop-bands and cloaking, all unfeasible in naturally occurring materials [3]. Waves in these materials can propagate only within certain frequency bands and are completely blocked within forbidden bandgaps [4, 5].

Frequency bandgaps can be caused by the presence of local resonators, which are normally either attached to the surface of the metamaterial structure or embedded inside [6]. Exhaustive research has already been carried out on design criteria and properties of metamaterial structures made of a single beam with local resonators [7, 8]. Frequency bandgaps in these metamaterial structures occur due to local resonators absorbing kinetic energy from the oscillations propagating through the metamaterial structure [9]. When the frequency of the external vibration and the resonant frequency of the local resonators coincide, energy from these vibrations transferrs to the local resonators [6]. On the other hand, the Bragg's scattering in the periodic structures also leads to generation of frequency bandgaps [10] due to the wavelengths of the Bragg scattering mechanism. The presence of local resonators makes it possible to generate bandgaps at much lower frequencies than the Bragg's frequencies [11, 12]. The related applications are promising in vibration insulators, frequency filters, waveguides and energy harvesting [9, 13, 14].

*Corresponding author
Email address: `gayane@liverpool.ac.uk` (G. Piliposian)

Waves propagating through beams may cause damages for the structures and inaccuracies for some experimental measurements. Especially important is the stability problem in structures which can be modelled as beams, for example, high-speed trains in a railway structure. To guarantee safety of high-speed trains, the mechanical properties of the train have to be chosen such that the instability is prevented. The stability problems of the vibration of a bogie uniformly moving along a Timoshenko beam on a viscoelastic foundation has been studied in [15], where it has been shown that the stability of the model largely depends on the damping in the supports and in the foundation. When the railway vehicle exceeds the minimum phase velocity of waves in the beam, which may lead to the vibration of the system becoming unstable, the stability problems have been investigated and instability intervals determined for varying parameters in [16–18].

Many engineering structures however are designed as one-dimensional periodically supported structures. Examples include railway tracks, pipelines and multi-span bridges [19, 20]. Dynamic behaviour of these structures are important for reducing their vibration response and failure, fatigue and damage and reducing the transmitted noise to the surrounding environment. Band gap concept have been used in several structural configurations for the control of the behaviour of waves in beams which are widely used in engineering constructions. The existence of multi-flexural band gaps can be exploited for the possibility of flexural vibration control of beams. Suppression of these vibrations in an Euler–Bernoulli beam with attached lateral local resonators is studied in [21]. It is shown that band gaps can be tuned by changing the geometry parameters and the spring constants of the resonators. The possibility of enlarging the bandwidth by changing the geometrical or material parameters is again revealed in [22]. Flexural waves in a periodic beam on elastic foundations are considered in [23], where it is shown that the presence of an elastic foundation can result also in a low frequency and wider range band gap.

If the periodicity of the metamaterial is infinite, the Bloch-Floquet theory is normally used to reduce the analysis of the wave propagation to the problem for a single unit cell [24]. When the periodic arrangement is confined within a finite spatial domain, the analysis becomes complicated [25]. Normally the transfer matrix approach with finite element method is more convenient for the investigation of finite periodic structures with boundary conditions imposed at the ends.

Most papers investigate wave propagation properties in an infinite periodic structure. However understanding the oscillatory behaviour through finitely periodic media is important for analyzing their acoustic properties, since the number of periodic cells is finite in most structures. In this paper we investigate forced vibrations of finite length multi span beams with periodically arranged intermediate external supports and internal hinges for qualitative and quantitative analysis of localization of flexible waves. Wave localization makes it possible to control the propagation of waves and can lead to many new applications [26]. On the other hand, localization can result in local energy concentrations which can affect the reliability and durability of engineering applications. In both scenarios, since small irregularities can cause substantial consequences, it is important to investigate the underlying physical mechanisms of wave and vibration localization. Stronger vibration localization leads to enhanced vibration energy harvesting capabilities [27]. To the best of the authors' knowledge, the strong localization of flexible waves in a finite periodic structure within the forbidden frequencies of band gaps caused by both forced vibrations and periodicity has not been reported before.

2. Statement of the problem

Consider an Euler-Bernoulli beam with one end $x = 0$ connected to a device driver that oscillates with an amplitude U_0 and frequency ω and the other end $x = L$ is pinned or free to vibrate. In the first problem in the meta beam region $x \in (a, L)$ at points $x = a + (n-1)d$, $(n = 1, 2, ...N)$ N

internal hinges are located at a distance d from each other. In the second problem at equal distance from internal hinges external intermediate supports are located (Fig.1).

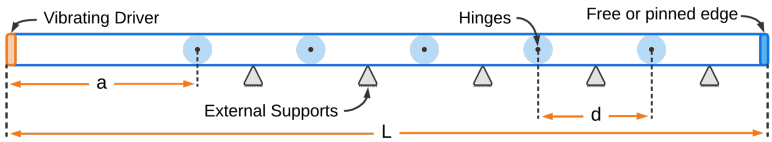

Fig. 1: Cantilevered beam with N periodically arranged hinges and external supports

The equation of motion of Euler-Bernoulli beam can be described by the following equation

$$EI\frac{\partial^4 W_\pm}{\partial x^4} + \rho F\frac{\partial^2 W_\pm}{\partial t^2} = 0, \tag{1}$$

where $W_\pm(x,t)$ is the dynamic deflection of the beam, E is the elastic modulus, I is the area moment of inertia, ρ is the bulk density, F is the cross-sectional area of the beam and subscript $(-)$ denotes the region $x \in (0,a)$, subscript $(+)$ denotes the region $x \in (a,L)$.

Forced vibrations in the beam can be generated by different ways. One of them is commonly used and technically easily realized oscillating driver connected to a fixed edge [28], where the following boundary conditions can apply [29]

$$W_-(0,t) = U_0\cos(\omega t), \quad \frac{\partial W_-(0,t)}{\partial x} = 0. \tag{2}$$

At the beam interface $x = a$ where the first internal hinge is placed the moments are equal to zero, the beam deflection and shear are continuous

$$\frac{\partial^2 W_-(a,t)}{\partial x^2} = 0, \quad \frac{\partial^2 W_+(a,t)}{\partial x^2} = 0, \tag{3}$$

$$W_+(a,t) = W_-(a,t), \quad \frac{\partial^3 W_+(a,t)}{\partial x^3} = \frac{\partial^3 W_-(a,t)}{\partial x^3}. \tag{4}$$

Conditions at the beam end and the interface conditions at points where periodic hinges or intermediate supports are located will be defined.

Writing $W_\pm(x,t) = U_\pm(x)\cos(\omega t)$, the amplitude functions $U_\pm(x)$ will satisfy the following equation

$$\frac{d^4 U_\pm}{dx^4} - p^4 U_\pm = 0, \quad \text{where} \quad p^4 = \frac{F\rho\omega^2}{EI}. \tag{5}$$

Satisfying boundary conditions (2) and the first boundary condition in (3), the solution in the meta-beam region $x \in (0,a)$ can be written as follows

$$U_-(x) = \frac{U_0(\cosh(ap)\cos(px) + \cos(ap)\cosh(px))}{\cos(ap) + \cosh(ap)}$$
$$+A_0\left(\frac{\sin(p(a-x)) + \sinh(ap)\cos(px) - \cosh(ap)\sin(px) - \cosh(px)(\sin(ap) + \sinh(ap))}{\cos(ap) + \cosh(ap)}\right.$$
$$\left. + \sinh(px)\right), \tag{6}$$

where the integration constant A_0 will be determined from the interface conditions at $x = a$.

In the periodic structure we will consider solutions in a basic unit cell $x \in (\beta_n - d, \beta_n)$, $\beta_n = a + nd,\ n = 1, 2, ...N)$.

Two periodic structures will be considered:

PH beam: a meta beam with periodically arranged N internal hinges which are placed at the end points of the unit cells $x = \beta_n - d$ and $x = \beta_n$.

PHS beam: a meta beam with periodically arranged N internal hinges and N intermediate external supports. The hinges are placed at the end points of the unit cells $x = \beta_n - d$, $x = \beta_n$ and the intermediate supports are placed at the middle of the unit cells $x = \beta_n - d/2$.

Interface conditions at points where the internal hinges are located starting from $x = a + d$ can be cast as

$$\frac{d^2U_+(x)}{dx^2} = 0, \quad \left[\frac{d^3U_+(x)}{dx^3}\right] = 0, \quad [U_+(x)] = 0. \tag{7}$$

Interface conditions at points where the external supports are located are

$$\left[\frac{d^2U_+(x)}{dx^2}\right] = 0, \quad \left[\frac{dU_+(x)}{dx}\right] = 0, \quad U_+(x) = 0. \tag{8}$$

In (7) and (8) $[\cdot]$ is a jump of a function across the interfaces.

3. Propagator matrix approach

3.1. Meta PH beam with periodically arranged internal hinges

In the basic unit cell the solution of the amplitude functions $U_+(x)$ from (5) satisfying the first boundary condition in (7) at $x = \beta_n$ and $x = \beta_n - d$ can be written as

$$\begin{aligned} U_+(x) = c_1 \left(\sin(p(\beta_n - x)) - g(x)\sin(dp)\right) \\ + c_2 \left(\sinh(p(\beta_n - x)) - g(x)\sinh(dp)\right), \end{aligned} \tag{9}$$

where

$$g(x) = \frac{\cos(p(\beta_n - x)) + \cosh(p(\beta_n - x))}{\cos(dp) - \cosh(dp)}, \tag{10}$$

and c_1 and c_2 are unknown constants.

Since the rest of interface contact conditions in (7) are imposed on the functions $U_+(x)$ and $\frac{d^3U_+(x)}{dx^3}$, it is convenient to introduce the following column vectors

$$\mathbf{U}_+(x) = \begin{pmatrix} U_+(x) \\ \dfrac{d^3U_+(x)}{dx^3} \end{pmatrix}, \quad \mathbf{C} = \begin{pmatrix} c_1 \\ c_2 \end{pmatrix}. \tag{11}$$

Using (9) the solution in the matrix form can be written as

$$\mathbf{U}_+(x) = \mathbf{P}(x)\mathbf{C}, \tag{12}$$

where

$$\mathbf{P}(x) = \begin{pmatrix} \sin(p(\beta_n - x)) - g(x)\sin(dp)) & \sinh(p(\beta_n - x)) - g(x)\sinh(dp) \\ p^3(\cos(p(\beta_n - x)) + f(x)\sin(dp)) & -p^3(\cosh(p(\beta_n - x)) + f(x)\sinh(dp)) \end{pmatrix}, \tag{13}$$

and

$$f(x) = \frac{\sin(p(\beta_n - x)) + \sinh(p(\beta_n - x))}{\cos(dp) - \cosh(dp)}. \tag{14}$$

A propagator matrix method can be used now to link the field values of the vectors $\mathbf{U}_+(\beta_n)$ and $\mathbf{U}_+(\beta_n - d)$ in the unit cell.

Since

$$\mathbf{U}_+(\beta_n) = \mathbf{P}(\beta_n)\mathbf{C} \quad \text{and} \quad \mathbf{U}_+(\beta_n - d) = \mathbf{P}(\beta_n - d)\mathbf{C}, \tag{15}$$

the vector $\mathbf{C}$ can be eliminated giving the following relation linking the vector field values within a unit cell

$$\mathbf{U}_+(\beta_n) = \mathbf{R}\mathbf{U}_+(\beta_n - d), \quad \mathbf{R} = \mathbf{P}(\beta_n)\mathbf{P}^{-1}(\beta_n - d), \tag{16}$$

where $\mathbf{R}$ is a unimodal propagator matrix, which links the field vectors at the ends of the n-th cell. Note that the elements of matrix $\mathbf{R}$ do not depend on the cell number:

$$\mathbf{R} = \begin{pmatrix} r_{11} & r_{12} \\ r_{21} & r_{22} \end{pmatrix}, \tag{17}$$

and

$$r_{11} = \frac{\sin(dp)\cosh(dp) - \cos(dp)\sinh(dp)}{\sin(dp) - \sinh(dp)}, \; r_{22} = r_{11}, \tag{18}$$

$$r_{12} = \frac{2\sin(dp)\sinh(dp)}{p^3(\sin(dp) - \sinh(dp))}, \; r_{21} = \frac{p^3(1 - \cos(dp)\cosh(dp))}{\sin(dp) - \sinh(dp)}. \tag{19}$$

The relation (16) will enable to establish a link between values of the vectors $U_+(a)$ and $U_+(L)$ and evaluate the relative deflections of the beam at any unit cell of the meta beam with periodically arranged internal hinges in proportion to meta beam deflection at point $x = a$.

3.2. ***Meta PHS beam with periodically arranged internal hinges and external intermediate supports***

Consider now a meta beam with periodically arranged N internal hinges and N intermediate supports. The hinges are placed at the end points of the unit cell $x = \beta_n - d, x = \beta_n$ and the intermediate supports are placed at the middle of the unit cells at points $x = \beta_n - d/2$ (Fig.1).

In the unit cell the solutions at the points where the hinges are placed and satisfying conditions

$$\frac{d^2U_{1+}(\beta_n)}{dx^2} = 0, \quad \frac{d^2U_{2+}(\beta_n - d)}{dx^2} = 0 \tag{20}$$

in both sides of the external intermediate supports can be cast as

$$U_{1+}(x) = C_1\sin(p(x - \beta_n)) + C_2\sinh(p(x - \beta_n)) + C_0(\cos(p(x - \beta_n)) - \cosh(p(x - \beta_n))), \tag{21}$$

$$U_{2+}(x) = A_1\sin(p(x - \beta_n + d)) + A_2\sinh(p(x - \beta_n + d)) + D_0(\cos(p(x - \beta_n + d)) - \cosh(p(x - \beta_n + d))). \tag{22}$$

From four interface conditions (8) it follows that

$$U_{1+}(\beta_n - d/2) = 0, \quad U_{2+}(\beta_n - d/2) = 0, \tag{23}$$

$$\frac{dU_{1+}(\beta_n - d/2)}{dx} = \frac{dU_{2+}(\beta_n - d/2)}{dx}, \quad \frac{d^2U_{1+}(\beta_n - d/2)}{dx^2} = \frac{d^2U_{2+}(\beta_n - d/2)}{dx^2} \tag{24}$$

the constants C_1, C_2, A_1 and A_2 can be expressed via C_0 and D_0 as follows

$$C_1 = D_0\psi\phi^{-1}\csc(dp/2) + C_0\theta\phi^{-1}, \quad C_2 = C_0\vartheta\phi^{-1} - D_0\mathrm{csch}(dp/2)\psi\phi^{-1}, \tag{25}$$

$$A_1 = -D_0\theta\phi^{-1} - C_0\csc(dp/2)\psi\phi^{-1}, \quad A_2 = C_0\psi\phi^{-1}\mathrm{csch}(dp/2) - D_0\vartheta\phi^{-1}, \tag{26}$$

where the following notations are made

$$\phi = 2(\cot(dp/2) - \coth(dp/2)), \quad \psi = \csc(dp/2) + \mathrm{csch}(dp/2), \tag{27}$$

$$\theta = 1 - \cot^2(dp/2) + 2\cot(dp/2)\coth(dp/2) + \csc(dp/2)\mathrm{csch}(dp/2), \tag{28}$$

$$\vartheta = 1 + \cot^2(dp/2) - 2\cot(dp/2)\coth(dp/2) - \csc(dp/2)\mathrm{csch}(dp/2). \tag{29}$$

It follows from (21), (22) and (25), (26) that

$$\mathbf{U}_{1+}(\beta_n) = \mathbf{P}_1\mathbf{C}_0, \qquad \mathbf{U}_{2+}(\beta_n - d) = \mathbf{P}_2\mathbf{C}_0, \tag{30}$$

where

$$\mathbf{U}_{1+}(\beta_n) = \begin{pmatrix} U_{1+}(\beta_n) \\ \dfrac{d^3U_{1+}(\beta_n)}{dx^3} \end{pmatrix}, \quad \mathbf{U}_{2+}(\beta_n - d) = \begin{pmatrix} U_{2+}(\beta_n - d) \\ \dfrac{d^3U_{2+}(\beta_n - d)}{dx^3} \end{pmatrix}, \quad \mathbf{C}_0 = \begin{pmatrix} C_0 \\ D_0 \end{pmatrix} \tag{31}$$

$$\mathbf{P}_1 = \phi^{-1}\begin{pmatrix} 0 & 2\phi \\ p^3\gamma\psi & p^3(\theta - \vartheta) \end{pmatrix}, \quad \mathbf{P}_2 = \phi^{-1}\begin{pmatrix} 2\phi & 0 \\ p^3(\vartheta - \theta) & -p^3\gamma\psi \end{pmatrix}, \tag{32}$$

and

$$\gamma = \csc(dp/2) + \mathrm{csch}(dp/2).$$

Now the vector $\mathbf{C}_0$ can be eliminated to obtain

$$\mathbf{U}_+(\beta_n) = \mathbf{Q}\mathbf{U}_+(\beta_n - d), \tag{33}$$

where

$$\mathbf{Q} = \mathbf{P}_1\mathbf{P}_2^{-1}, \quad \mathbf{U}_+(\beta_n) = \mathbf{U}_{1+}(\beta_n), \quad \mathbf{U}_+(\beta_n - d) = \mathbf{U}_{2+}(\beta_n).$$

Matrix $\mathbf{Q}$ is a unimodal propagator matrix of the wave field for the Euler–Bernulli metastructure beam, which connects the vectors $\mathbf{U}_+(\beta_n)$ and $\mathbf{U}_+(\beta_n - d)$ at the ends of the n-th cell where internal hinges are placed.

Elements of matrix $\mathbf{Q}$ can be expressed as

$$p_{11} = \frac{\cosh(dp) - \cos(dp) - 4\sin(dp/2)\sinh(dp/2) - 2\sin(dp)\sinh(dp)}{2(\sin(dp/2) + \sinh(dp/2))^2}, \quad p_{22} = p_{11}$$

$$p_{12} = \frac{4\sin(dp/2)\sinh(dp/2)(\sin(dp/2)\cosh(dp/2) - \cos(dp/2)\sinh(dp/2))}{p^3(\sin(dp/2) + \sinh(dp/2))^2}, \tag{34}$$

$$p_{21} = -\frac{2p^3(\cos(dp/2)\cosh(dp/2) + 1)(\sin(dp/2)\cosh(dp/2) - \cos(dp/2)\sinh(dp/2))}{(\sin(dp/2) + \sinh(dp/2))^2}.$$

The relation (33) will be used to establish a relationship between vectors $U_+(a)$ and $U_+(L)$ and evaluate the deflections of the beam at any unit cell of meta beam with periodically arranged internal hinges and external supports in proportion to the deflection at the starting point $x = a$.

3.3. ***Solutions for the relative deflections and "shear" functions***

If $\mathbf{M}$ is a unimodal matrix, where $\mathbf{M}$ stands for matrices $\mathbf{R}$ or $\mathbf{Q}$, then in the region of the meta beam where the hinges and external supports are located the unimodal propagator matrix $\mathbf{M}^n$ linking the vectors at points $x = a$ and $x = a + nd$ can be constructed by repeating (16) or (33) n times:

$$\mathbf{U}_+(a + nd) = \mathbf{M}^n \mathbf{U}_+(a). \tag{35}$$

Since $\mathbf{M}^{N-n}\mathbf{U}_+(a + nd) = \mathbf{M}^N \mathbf{U}_+(a) = \mathbf{U}_+(a + Nd)$ the vectors can be linked at $x = a + Nd = L$ and $x = a + (n - 1)d$ in the following way

$$\mathbf{M}^{N-n+1}\mathbf{U}_+(a + (n - 1)d) = \mathbf{U}_+(L). \tag{36}$$

According to Sylvester's matrix polynomial theorem [30] the elements of the n-th power of a 2×2 unimodal matrix $\mathbf{M} = \{m_{ij}\}_{i,j=1}^2$ can be expressed as

$$\mathbf{M}^n = \begin{pmatrix} M_{11}(n) & M_{12}(n) \\ M_{21}(n) & M_{22}(n) \end{pmatrix}, \tag{37}$$

where

$$\begin{aligned} &M_{11}(n) = m_{11}S_{n-1} - S_{n-2}, \;\; M_{12}(n) = m_{12}S_{n-1}, \\ &M_{21}(n) = m_{21}S_{n-1}, \;\; M_{22}(n) = m_{22}S_{n-1} - S_{n-2}, \end{aligned} \tag{38}$$

and $S_n(\eta)$ are the Chebyshev polynomials of second kind, namely

$$S_n(\eta) = \frac{\sin((n + 1)\arccos(\eta))}{\sin(\arccos \eta)}, \;\; \eta = \frac{m_{11} + m_{22}}{2}. \tag{39}$$

In vector notations the interface condition (4) at $x = a$ can be written as

$$\mathbf{U}_+(a) = \mathbf{U}_-(a), \;\; \text{where} \;\; \mathbf{U}_-(a) = \begin{pmatrix} U_-(a) \\ \dfrac{d^3U_-(a)}{dx^3} \end{pmatrix}. \tag{40}$$

If follows from (35) and (40) that the unknown constant A_0 can be determined from the following matrix equation

$$\mathbf{M}^N \mathbf{U}_+(a) = \mathbf{U}_+(L), \tag{41}$$

where

$$\mathbf{U}_+(a) = \begin{pmatrix} \dfrac{2A_0(\cos(ap)\sinh(ap) - \sin(ap)\cosh(ap))}{\cos(ap) + \cosh(ap)} + \dfrac{2U_0\cos(ap)\cosh(ap)}{\cos(ap) + \cosh(ap)} \\ \dfrac{2A_0p^3(\cos(ap)\cosh(ap) + 1)}{\cos(ap) + \cosh(ap)} + \dfrac{p^3U_0(\cos(ap)\sinh(ap) + \sin(ap)\cosh(ap))}{\cos(ap) + \cosh(ap)} \end{pmatrix}. \tag{42}$$

For a PHS beam both free edge and pinned edge at x=L can be considered. Since a PH beam cannot have a free edge, for this beam only pinned edge at x = L is considered [31], [32].

In the case of the free edge

$$\frac{d^2U_+(L)}{dx^2} = 0, \;\; \frac{d^3U_+(L)}{dx^3} = 0, \;\; \mathbf{U}_+(L) = \begin{pmatrix} U_+(L) \\ 0 \end{pmatrix}. \tag{43}$$

For a pinned edge beam

$$\frac{d^2U_+(L)}{dx^2} = 0,\ \ U_+(L) = 0, \mathbf{U}_+(L) = \begin{pmatrix} 0 \\ f(L) \end{pmatrix}, \tag{44}$$

where $f(x) = \dfrac{d^3U_+(x)}{dx^3}$ is the beam's "shear" function and in (43) and (44) $U_+(L)$ and $f(L)$ are unknown displacement and "shear" which need to be determined from the interface condition given at $x = a$.

In the case of a free edge beam the constants A_0 and $U_+(L)$ can be determined from the equation

$$\begin{pmatrix} M_{11}(N) & M_{12}(N) \\ M_{21}(N) & -M_{22}(N) \end{pmatrix} \mathbf{U}_+(a) = \begin{pmatrix} U_+(L) \\ 0 \end{pmatrix}. \tag{45}$$

It follows that

$$\mathbf{U}_+(a) = M_{22}(N)U_+(L),\ \ f(a) = -M_{21}(N)U_+(L), \tag{46}$$

where

$$U_+(L) = U_0\Delta_1^{-1}(\cos(ap) + \cosh(ap)), \tag{47}$$

$$\Delta_1 = M_{21}p^{-3}(\cos(ap)\sinh(ap) - \sin(ap)\cosh(ap)) + M_{22}(\cos(ap)\cosh(ap) + 1). \tag{48}$$

The equation $\Delta_1(\omega) = 0$ defines the bands of resonance frequencies of a beam with a free edge at $x = L$. From (43) it follows that

$$U_+(a + d(n-1)) = M_{22}(N - n + 1)U_+(L),\ \ f(a + d(n-1)) = -M_{21}(N - n + 1)U_+(L). \tag{49}$$

Taking into account that $m_{11} = m_{22} = \eta$ and

$$M_{22}(n) = \eta S_{n-1}(\eta) - S_{n-2}(\eta) = T_n(\eta), \tag{50}$$

where $T_n(\eta)$ is the Chebyshev polynomials of first kind and $M_{21}(n) = m_{21}S_{n-1}$, we can define the relative displacement and relative "shear" at any unit cell of the periodic part of the beam in the following way

$$\tilde{U}_n = \frac{U_+(a + d(n-1))}{U_+(a)} = \frac{T_{N-n+1}(\eta)}{T_N(\eta)},\ \ \tilde{f}_n = \frac{f(a + d(n-1))}{f(a)} = \frac{S_{N-n}(\eta)}{S_{N-1}(\eta)}. \tag{51}$$

In the case of a pinned edge beam the constants A_0 and $f(L)$ will be determined from the following equation

$$\begin{pmatrix} M_{11}(N) & M_{12}(N) \\ M_{21}(N) & -M_{22}(N) \end{pmatrix} \mathbf{U}_+(a) = \begin{pmatrix} 0 \\ f(L) \end{pmatrix}, \tag{52}$$

and from (46)

$$f(a) = M_{11}(N)f(L),\ \ U_+(a) = -M_{12}(N)f(L), \tag{53}$$

where

$$f(L) = -U_0p^3\Delta_2^{-1}(\cos(ap) + \cosh(ap)), \tag{54}$$

$$\Delta_2 = M_{11}(\cos(ap)\sinh(ap) - \sin(ap)\cosh(ap)) + M_{12}p^3(\cos(ap)\cosh(ap) + 1). \tag{55}$$

The equation $\Delta_2(\omega) = 0$ defines the bands of resonance frequencies of the beam with pinned edge at $x = L$.

It follows from (26) that

$$U_+(a+d(n-1)) = M_{12}(N-n+1)U_+(L),\;\; f(a+d(n-1)) = M_{11}(N-n+1)U_+(L). \tag{56}$$

Thus in this case

$$\tilde{U}_n = \frac{U_+(a+d(n-1))}{U_+(a)} = \frac{S_{N-n}(\eta)}{S_{N-1}(\eta)},\;\; \tilde{f}_n = \frac{f(a+d(n-1))}{f(a)} = \frac{T_{N-n+1}(\eta)}{T_N(\eta)}. \tag{57}$$

In (51) and (57) $\tilde{U}_n$ and $\tilde{f}_n$ define relative deflections and "shear" of any unit cell of the periodic part of the meta-beam in proportion to the meta-beam deflection and "shear" at point $x = a$.

3.4. ***Solution of the problem for infinite periodic beams***

Applying the Bloch -Floquet periodicity condition $\mathbf{U}_0(\beta_n) = \lambda \mathbf{U}_0(\beta_n - d)$ at both ends of the unit cell results in the following eigenvalue problem

$$(\mathbf{M} - \lambda \mathbf{I})\mathbf{U}_+(\beta_n) = 0, \tag{58}$$

where $\mathbf{M}$ stands for matrix $\mathbf{R}$ for a meta beam with periodically arranged internal hinges and $\mathbf{Q}$ for a meta beam with periodically arranged internal hinges and external intermediate supports, $\mathbf{I}$ is a 2×2 identity matrix, $\lambda = \exp(ikd)$ and k is the the Bloch–Floquet wave number. It follows from (58) that the eigenvalues of the periodic structure satisfy the following equation:

$$1 - 2\lambda m_{11} + \lambda^2 = 0. \tag{59}$$

It follows from (59) that $\cos kd = m_{11}$, and, since $m_{11} = \eta$, the equation defining the gaps of the infinite beam with internal hinges can be found from

$$\cos(kd) = \frac{\sin(dp)\cosh(dp) - \cos(dp)\sinh(dp)}{\sin(dp) - \sinh(dp)}. \tag{60}$$

The equation defining the gaps of the infinite beam with internal hinges and supports can be written as

$$\cos(kd) = \frac{\cosh(dp) - \cos(dp) - 4\sin\left(\frac{dp}{2}\right)\sinh\left(\frac{dp}{2}\right) - 2\sin(dp)\sinh(dp)}{2\left(\sin\left(\frac{dp}{2}\right) - \sinh\left(\frac{dp}{2}\right)\right)^2}. \tag{61}$$

Thus by virtue of properties of a unimodal propagator matrix defined in sections 3.1 and 3.2 for the solution of a finite length periodic structure we determined the band gaps of counterpart infinite periodic structure.

4. Analysis and conclusions

It follows from (60) and (61) that the condition $|\eta| > 1$ defines band gaps in an infinite metastucture beams. Dispersion curves defining band gaps in the first Brillouin zone, are presented in Figure 2, where $\Omega = \omega d^2\sqrt{(EI)^{-1}\rho A}$ is a dimensionless bending frequency of the metastructure. For a beam with periodically arranged hinges (PH) dashed horizontal lines on dispersion curves (Fig. 2a) determine bounds of the first gap $\Omega \in (22.37, 39.43)$, the second and third gaps $\Omega \in (61.62, 88.73)$ and $\Omega \in (120.78, 157.75)$, respectively (also shown as black dots on Fig. 7). There is also a cut-off

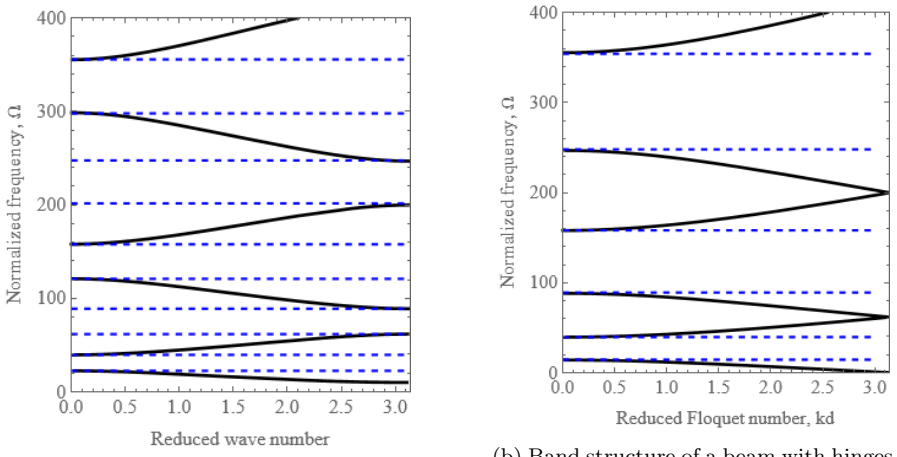

(a) Band structure of a beam with hinges

(b) Band structure of a beam with hinges and external supports

Fig. 2: Dispersion curves.

frequency at $\Omega = 9.6$ below which the waves cannot propagate. For the beam with periodically arranged hinges and external suppers (PHS) the bounds of frequency ranges which determine the band gaps are $\Omega \in (14.65, 39.5)$, $\Omega \in (88.1, 157.7)$, $\Omega \in (248.3, 351.9)$, respectively (Fig. 2b). Within the same frequency range the band gaps in this case are fewer but wider and there is no a frequency cut-off.

Dependence of the deviation $|\eta|$ on the dimensionless frequency Ω is presented in Figure 3. For a PH beam the parameter $|\eta|$ takes the same maximal values $|\eta|_{max}(\Omega) = 1.404$ in the middle of the band gaps, which are the points where $|\eta| > 1$. In particular at $\Omega = 30.9$ for the first band gap. For the beam with periodically arranged hinges and external supports the maximum values of $|\eta|$ are different and higher, in particular $|\eta|_{max}(\Omega) = 2.24$, $|\eta|_{max}(\Omega) = 3.05$ and $|\eta|_{max}(\Omega) = 2.95$ for first, second and third gaps, respectively.

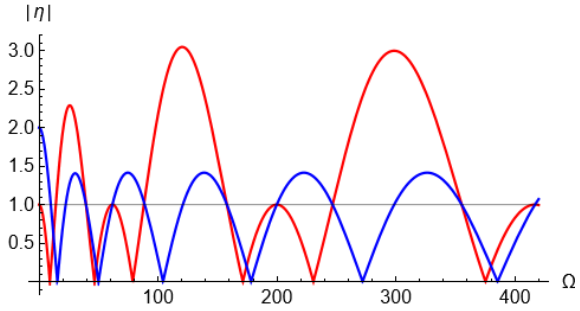

Fig. 3: Graphs of deviation functions $|\eta|$. The blue and red curves show the band structure of a beam with periodically arranged hinges and a beam with periodically arranged hinges and external supports.

The relative functions $\tilde{U}_n$ and $\tilde{f}_n$ are described by Chebyshev polynomials $T_n(\eta)$ and $S_n(\eta)$. Figure 4 shows the graphs of $\tilde{T}_n = T_{N-n+1}(\eta)/T_n(\eta)$ and $\tilde{S}_n = S_{N-n+1}(\eta)/S_n(\eta)$ for values of $\eta > 1$ and $\eta < 1$. The two curves practically coincide even at $\eta = 1.05$ and $N = 10$, whereas the values of these curves diverge already at $\eta = 0.95$. Since for $|\eta| > 1$ the functions $\tilde{T}_n$ and $\tilde{S}_n$ practically coincide, all results which are presented below for relative deflection function are valid also for the relative "shear" for both a PH beam with a pinned edge and a PHS beam with free or pinned edges.

Figure 5 shows the relative deflection $\tilde{U}_n$ as a function of the number of cells n for both PH and PHS beams with free and pinned edges for $N = 20$. The values are calculated at the mid point $\Omega = 30.9$ ($|\eta| = 1.404$) of the first band gap for the PH beam (the red lines), at the mid point

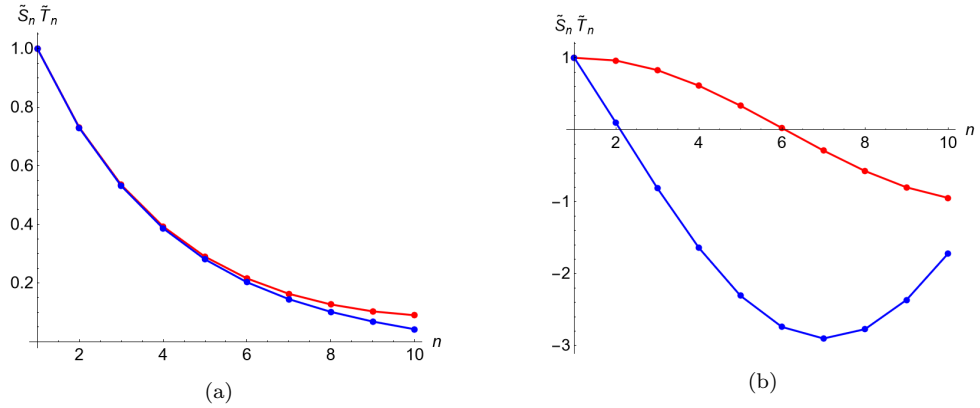

Fig. 4: Functions $\tilde{T}_n = T_{N-n+1}(\eta)/T_n(\eta)$ (red curve) and $\tilde{S}_n = S_{N-n+1}(\eta)/S_n(\eta)$ (blue curve) for (a) $\eta = 1.05$, (b) $\eta = 0.95$.

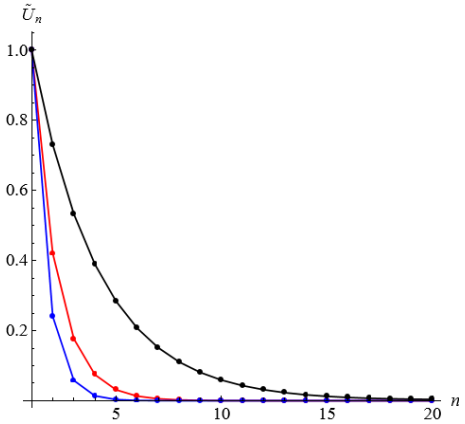

Fig. 5: Relative deflections for N=20 (a) for a PH (red lines) and a PHS (blue lines) beams at the middle of the first frequency band gap.

$\Omega = 25.7$ ($|\eta| = 2.02$) of the first band gap for the PHS beam (the blue lines). The black lines show values of the relative deflection $\tilde{U}_n$ at points close to the first gap boundaries, where $|\eta| = 1.05$ for both PH and PHS beams. The graphs show that a strong localization (displacement and "shear" attenuation) of a flexible wave occurs when the frequency of the forced vibration coincides with the midpoint frequency of the first band gap even for the number of cells as few as $N = 10$. Moreover there is a stronger localization of acoustic flexible waves in the case of a PHS beam compared to a PH beam. Figure 4b confirms that outside the band gaps a localization of the relative displacement and "shear " does not occur at the forced vibration frequencies .

Since $\dfrac{T_{n-1}(\eta)}{T_n(\eta)} \approx 0.41$ for $\eta = 1.404$, for a PH beam and $\dfrac{T_{n-1}(\eta)}{T_n(\eta)} \approx 0.23$ for $\eta = 2.2$, $(n > 2)$ for the PHS beam, the discrete function $\tilde{U}$ can be approximated with high accuracy at the middle frequency of the first band gap by a continuous function as follows

$$\frac{T_{N-n+1}(\eta)}{T_N(\eta)} \sim Q(\alpha) = 0.41^{N\alpha} \quad \text{and} \quad Q(\alpha) = 0.23^{N\alpha}. \tag{62}$$

for PH and PHS beams defined in interval $\alpha = (x-a)/(L-a)$, $x \in (a, L-a)$. This can be used to compare the localisation of waves for different number of cells of the same length beam.

Figure 6 shows the variation of the relative deflection $\tilde{U}_n \sim Q(\alpha)$ along the beam's periodic part for $N = 5$, $N = 10$ and $N = 20$ for the same length of the beam L. The dot points on the curve for

$N = 10$ corresponding to the exact values of the relative deflection confirm the high accuracy of the approximation of the function $Q(\alpha)$. Analysis of these curves shows that the localization of acoustic flexible waves significantly increases with increasing number of hinges and supports. Moreover there is stronger localization of acoustic flexible waves for a PHS beam compared to a PH beam.

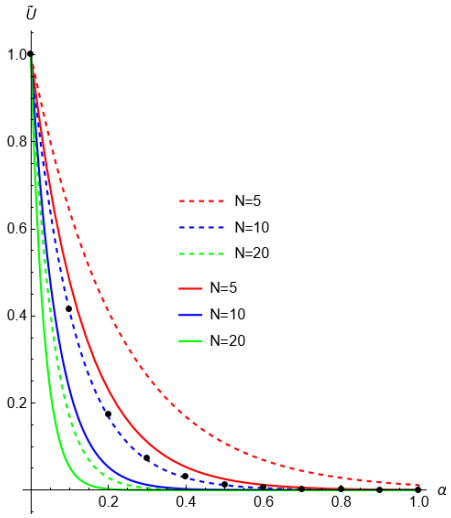

Fig. 6: Continuous approximation functions of the discrete relative deflection for (a) a meta beam with periodically arranged internal hinges (Solid lines) $Q(\alpha) = 0.41^{N\alpha}$ and (b) with periodically arranged internal hinges and external intermediate supports (dashed lines) $Q(\alpha) = 0.23^{N\alpha}$ for different number of cells.

In the problem of a wave propagation in a periodic infinite structure a very slight deviation of the parameter $|\eta|$ from 1 results in the wave band gap formation. However it follows from Figure 5 that in the finite periodic structures it is more important a large deviation of the parameter $|\eta|$ from 1, since a stronger localization happens for the PHS beam, for which the values of η are much larger than than for the PH beam (Fig. 3).

The results show that the localization of amplitudes of meta-baem displacements takes place only near the interface of the first cells. The flexible wave can not freely travel via periodic structure at frequencies within forbidden bands and are practically localized at the neighborhood of the first periodic cells. This effect takes place already at $N = 10$. This localization effect is very close to some results of wave localization in finite periodic structure discussed in [33] and [34].

Figures 7 and 9 show the graphs of the function $\Delta(\Omega)$, (zeros of which define resonance frequencies), for both a PH beam with a pinned edge and a PHS beam with a free or pinned edge within the first and second frequency gaps. The black dot points on the Ω axis are the bounds of these frequency gaps. For a comparative analysis the graphs of the function $\Delta(\Omega)$ on Figure 10 are presented within the range $0 < \Omega < 200$ for a PH beam with a pinned edge for $N = 10$ and $N = 1$.

The analysis of data on Figures 7-10 shows that increasing the number of hinges and supports significantly increases the number of zeroes of resonance frequencies outside the band gaps, but within the gaps it does not change the location and the number of zeroes, which are located mostly outside the frequency gaps. There are only a few zeroes of the resonance frequency within the frequency gaps. Due to the periodicity there exist anti-resonance frequencies outside the forbidden gaps at which the displacements approach to zero. Within the gaps in the PHS beam the locations of zeroes of the resonance frequency are slightly different for pinned and free edge boundary cases. The same results are expected to be valid in the range of the subsequent gaps.

The main results can be summarized as follows

1. The PH and PHS structures in the homogeneous infinite beam can open wide frequency

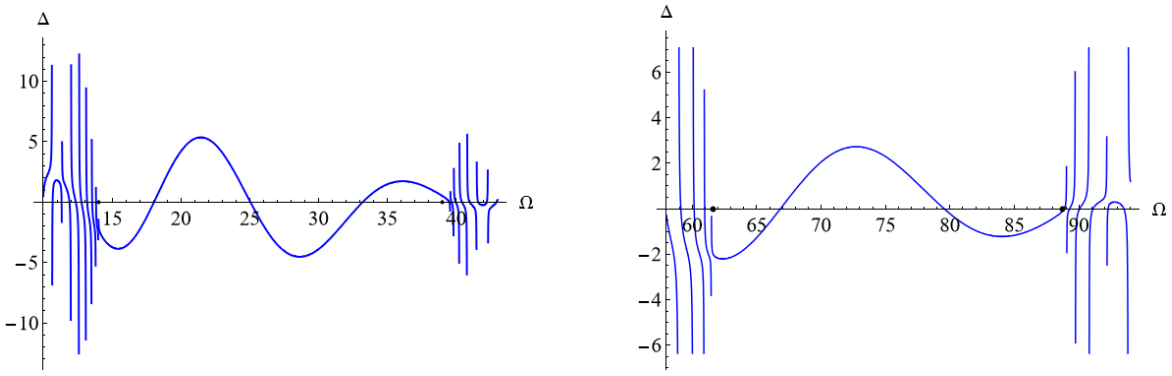

(a) (PH beam) First gap. (b) (PH beam) Second gap.

Fig. 7: Graphs of the function $\Delta(\Omega)$ for the PH beam with pinned edge, first and second gaps, $a = 4d$, $N = 20$.

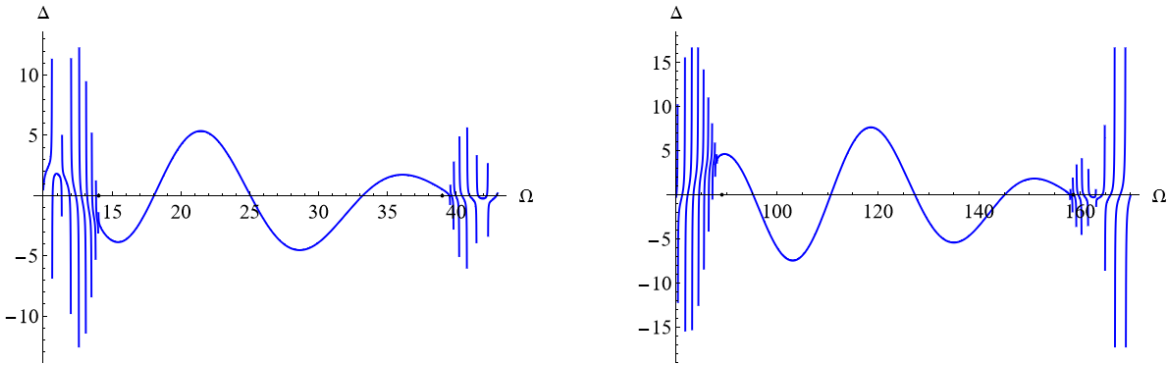

(a) (PHS beam) First gap (b) (PHS beam) Second gap

Fig. 8: Graphs of the function $\Delta(\Omega)$ for the PHS beam with a pinned edge for $a = 4d$, $N = 20$.

band gaps. Within the same frequency range the band gaps for PHS beams are fewer and wider and unlike the PH beam there is no a cut-off frequency below which waves cannot propagate.

2. In the problem of forced vibration of PH and PHS beams localization of flexible waves occurs when the frequencies of forced vibrations coincide with the "forbidden" frequencies of band gaps. The strong localization occurs at the mid frequencies of the band gaps. The localization takes place even in the case of small number of hinges and supports. The number of hinges and supports essentially increases the localization of acoustic flexible waves.

3. A beam with periodically arranged internal hinges and external intermediate supports demonstrates stronger localization of acoustic flexible waves compared to a beam with only periodically arranged internal hinges.

4. Due to periodicity there exist the anti-resonance frequencies outside of forbidden gaps at which the displacements approach to zero.

5. At frequencies within forbidden band gaps where a flexible wave cannot freely travel via periodic structure it is practically localized at the neighborhood of the first periodic cells.

6. Localization of acoustic flexible waves significantly depends on the number of hinges and external supports. The localization is stronger for larger numbers of hinges and external supports.

7. The resonance frequencies are mostly outside the forbidden frequency band gaps for both a beam with periodically arranged internal hinges and external intermediate supports and a beam with only periodically arranged internal hinges.

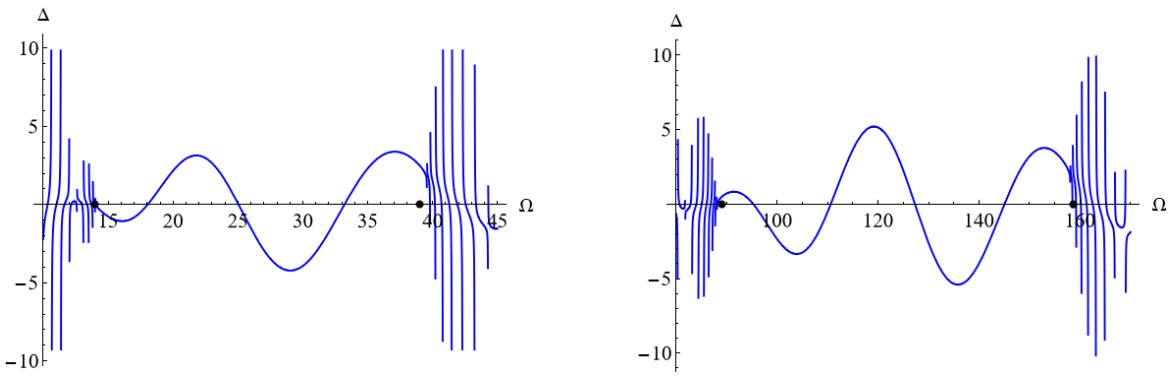

(a) (PHS beam) First gap (b) (PHS beam) Second gap

Fig. 9: The function $\Delta(\Omega)$ for the PHS beam with a free edge for $a = 4d$, $N = 20$.

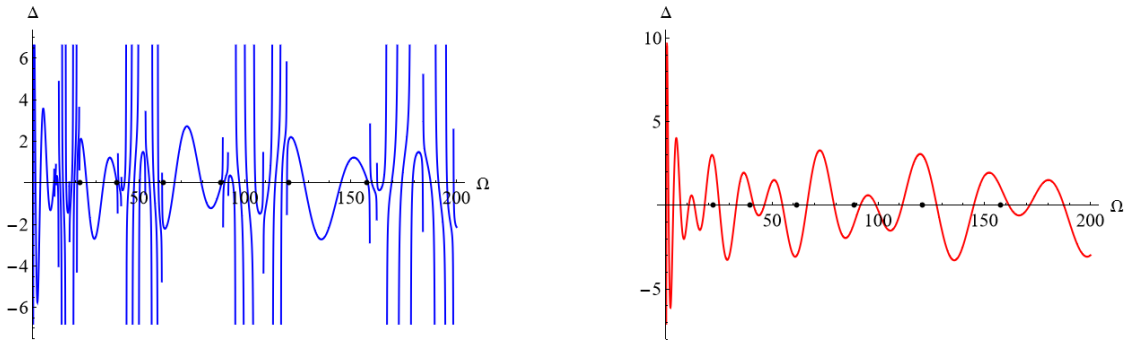

(a) (b)

Fig. 10: The function $\Delta(\Omega)$ in frequency range $0 < \Omega < 200$ for a PH beam with a pinned edge for $a = 4d$, (a) N=10, (b) N=1.

Acknowledgments

The work was supported by the State Committee of Science of RA, in the framework of the research project 21T-2C299.

References

[1] Wang, Z., Zhang, Q., Zhang, K., and Hu, G. (2016). Tunable Digital Metamaterial for Broadband Vibration Isolation at Low Frequency. Adv. Mater. Vol. 28(44), pp. 9857, 9861.

[2] Casablanca, O., Ventura, G., Garescì, F., Azzerboni, B., Chiaia, B., Chiappini, M., et al. (2018). Seismic Isolation of Buildings Using Composite Foundations Based on Metamaterials. J. Appl. Phys. 123 No. 17.

[3] Matlack, K. H., Bauhofer, A., Krödel, S., Palermo, A., and Daraio, C. (2016). Composite 3D-Printed Metastructures for Low-Frequency and Broadband Vibration Absorption. Proc. Natl. Acad. Sci. USA Vol. 113(30), pp. 8386-8390.

[4] Adams, S., Craster R.V., Guenneau S. (2008). Bloch waves in periodic multi-layered acoustic layers, Proceedings of the Royal Society of London A: Mathematical, Physical and Engineering Sciences. Vol. 464. No. 2098.

[5] Hussein M.I., Leamy M.J., Ruzzene M. (2014). Dynamics of phononic materials and structures: historical origins, recent progress, and future outlook, Applied Mechanics Reviews, 66, 040802/1-38.

[6] Anigbogu, W., Nguyen, H. and Bardaweel, H.(2021). Layered Metamaterial Beam Structures With Local Resonators for Vibration Attenuation: Model and Experiment. Frontiers in Mechanical Engineering, Vol. 7, p.768508.

[7] Liu, Z., Zhang, X., Mao, Y., Zhu, Y. Y., Yang, Z., Chan, C. T., et al. (2000). Locally Resonant Sonic Materials. Science, 289. 1734–1736.

[8] Failla,G., Santoro R., Burlon A., Russillo A. (2020). An exact approach to the dynamics of locally-resonant beams, Mechanics Research Communications, Vol. 103, 103460.

[9] Li, Y., Baker, E., Reissman, T., Sun, C., and Liu, W. K. (2017). Design of Mechanical Metamaterials for Simultaneous Vibration Isolation and Energy Harvesting. Appl. Phys. Lett. 111 (25), 251903.

[10] Kushwaha, M. S., Halevi, P., Dobrzynski, L., and Djafari-Rouhani, B. (1993). Acoustic Band Structure of Periodic Elastic Composites. Phys. Rev. Lett. 71 (13), 2022–2025.

[11] Liu, Z., Chan, C. T., and Sheng, P. (2005). Analytic Model of Phononic Crystals with Local Resonances. Phys. Rev. B 71 No.1, 14103.

[12] Botshekan M., Tootkaboni M., Louhghalam A. (2019). On the dynamics of periodically restrained flexural structures under moving loads, International Journal of Solids and Structures, Vol. 180–181, pp. 62-71,

[13] Piliposian G., Hasanyan A., Piliposyan G., Jilavyan H. (2020). On the Sensing, Actuating and Energy Harvesting Properties of a Composite Plate with Piezoelectric Patches, International Journal of Precision Engineering and Manufacturing-Green Technology, Vol.7, pp. 657–668.

[14] Reichl, K. K., and Inman, D. J. (2017). Lumped Mass Model of a 1D Metastructure for Vibration Suppression with no Additional Mass. J. Sound Vibration Vol. 403 pp. 75–89.

[15] Verichev S.N., Metrikine A.V. (2002). Instability of a Bogie moving on a flexible supported Timoshenko beam, Journal of Sound and Vibration, Vol.253(3), pp. 653-668.

[16] Stojanovic V., Petkovi M.D., Deng J. (2018). Stability of vibrations of a moving railway vehicle along an infinite complex three-part viscoelastic beam/foundation system, Int. Journal of Mechanical Sciences, Vol. 136, pp. 155-168.

[17] Stojanović V., Marko D. P., Deng J. (2018). Instability of vehicle systems moving along an infinite beam on a viscoelastic foundation, European Journal of Mechanics - A/Solids, Vol. 69, pp. 238-254.

[18] Stojanović V., Marko D. P., Deng J. (2019). Stability and vibrations of an overcritical speed moving multiple discrete oscillators along an infinite continuous structure, European Journal of Mechanics - A/Solids, Vol. 75, pp. 367-380.

[19] Gry L., Gontier C. (1997). Dynamic Modelling of Railway Track: A Periodic Model Based on a Generalized Beam Formulation, Journal of Sound and Vibration, Vol. 199(4), pp. 531-558,

[20] García-Palacios J., Samartín A., Melis M. (2012). Analysis of the railway track as a spatially periodic structure. Proc. of the Institution of Mechanical Engineers, Part F: Journal of Rail and Rapid Transit. 226(2), pp.113-123.

[21] Wang T., Sheng M.P., Qin Q.-H. (2016). Multi-flexural band gaps in an Euler–Bernoulli beam with lateral local resonators, Physics Letters A, Vol. 380(4), pp. 525-529.

[22] Xiang H.J., Shi Z.-F. (2009). Analysis of flexural vibration band gaps in periodic beams using differential quadrature method, Computers and Structures, Vol. 87(23–24), pp. 1559-1566.

[23] Yu D., Wen J., Shen H., Xiao Y., Wen X. (2012). Propagation of flexural wave in periodic beam on elastic foundations, Physics Letters A, Vol.376(4), pp. 626-630.

[24] Chen J., Chao I., Chen T. (2022). Bandgaps for flexural waves in infinite beams and plates with a periodic array of resonators, Journal of Mechanics, Vol 38, pp. 376–389.

[25] Kobayashi, F., Biwa, S. and Ohno, N. (2004). Wave transmission characteristics in periodic media of finite length: multilayers and fiber arrays. International journal of solids and structures, 41(26), pp.7361-7375.

[26] Chen Z., Y. Yang, Z Lu, Y Luo, (2013). Broadband characteristics of vibration energy harvesting using one-dimensional phononic piezoelectric cantilever beams. Physica B: Condensed Matter 410, pp. 5-12.

[27] Ma, T. X., Fan, Q. S., Zhang, C., Wang, Y. S. (2022). Flexural wave energy harvesting by the topological interface state of a phononic crystal beam. Extreme Mechanics Letters, 50, 101578.

[28] Romaszko M., Sapiński B., Sioma, A. (2015). Forced vibrations analysis of a cantilever beam using the vision method. Journal of Theoretical and Applied Mechanics, 53(1), pp.243-254.

[29] C. E. Repetto and A. Roatta and R. J. Welti, 2012. Forced vibrations of a cantilever beam, European Journal of Physics. Vol 33(5), p. 1187.

[30] Tovar, A.A. and Casperson, W., (1995). Generalized Sylvester theorems for periodic applications in matrix optics, J. Opt. Soc. Am. A 12, p.578-590.

[31] Wang C.Y., (2002). Buckling of an internally hinged column with an elastic support. Engineering Structures, Vol 24(10), pp.1357-1360.

[32] Lee, Y.Y., Wang, C.M. and Kitipornchai, S., 2003. Vibration of Timoshenko beams with internal hinge. Journal of engineering Mechanics, 129(3), pp.293-301.

[33] Piliposyan, D., Ghaz aryan, K., Piliposian, G. (2022). Localization of electro-elastic shear waves in a periodically stratified piezoelectric structure. Journal of Sound and Vibration, vol.536, 117142.

[34] Ghazaryan, K. B., Ghazaryan, R. A., Papyan, A. A., Ohanyan, S. K. (2020). Localisation of guided wave in stratified elastic reflector sandwiched between two elastic semi-spaces. Journal of Physics, vol. 1474(1), 012015.